Riemannian geometry of thermodynamics and systems with repulsive power-law interactions

George Ruppeiner
Division of Natural Sciences, New College of Florida, 5700 North Tamiami Trail, Sarasota, Florida 34243, USA
(Received 27 July 2004; revised manuscript received 29 April 2005; published 19 July 2005)

A Riemannian geometric theory of thermodynamics based on the postulate that the curvature scalar R is proportional to the inverse free energy density is used to investigate three-dimensional fluid systems of identical classical point particles interacting with each other via a power-law potential energy $\gamma r^{-\alpha}$. Such systems are useful in modeling melting transitions. The limit $\alpha \to \infty$ corresponds to the hard sphere gas. A thermodynamic limit exists only for short-range ($\alpha > 3$) and repulsive ($\gamma > 0$) interactions. The geometric theory solutions for given $\alpha > 3$, $\gamma > 0$, and any constant temperature T have the following properties: (1) the thermodynamics follows from a single function $b(\rho T^{-3/\alpha})$, where ρ is the density; (2) all solutions are equivalent up to a single scaling constant for $\rho T^{-3/\alpha}$, related to γ via the virial theorem; (3) at low density, solutions correspond to the ideal gas; (4) at high density there are solutions with pressure and energy depending on density as expected from solid state physics, though not with a Dulong-Petit heat capacity limit; (5) for $3 < \alpha < 3.7913$, the solution goes from the low to the expected high density limit smoothly; (6) for $\alpha > 3.7913$ a phase transition is required to go between these regimes; (7) for any $\alpha > 3$ we may include a first-order phase transition, which is expected from computer simulations; and (8) if $\alpha \to \infty$, the density approaches a finite value as the pressure increases to infinity, with the pressure diverging logarithmically in the density difference.

DOI: 10.1103/PhysRevE.72.016120 PACS number(s): 05.70.−a, 05.40.−a, 64.10.+h

I. INTRODUCTION

The basic laws of equilibrium thermodynamics have long achieved a venerable place in physics as being complete [1]. However, when one adds thermodynamic fluctuations to the picture, things are not so clear. It has been suggested [2,3] that fundamentally new results come from a Riemannian geometry with a metric based on thermodynamic fluctuation probabilities. The associated Riemannian curvature scalar is a measure of interaction strength, and yields fundamental information about thermodynamic systems through a postulate: *the curvature is inversely proportional to the inverse of the free energy density* [3,4].

This postulate may be expressed as a partial differential equation for the free energy density. Although this equation stands ready to deal with great complexity, the solution process is considerably simplified if we can find a method of reduction to an ordinary differential equation. In the application to critical phenomena, this was done by the substitution of a generalized homogeneous function [4]. Here, the substitution is inspired by the integral equations of state and the assumption of power-law inter-atomic interaction potential energies. A special case of this solution method, the self-gravitating gas, was considered previously [5], and this paper represents a generalization of that effort. Here, however, I emphasize repulsive interactions, which offer a regime where we may compare the geometric theory with statistical mechanics.

The basic philosophy of the geometric theory is the calculation of thermodynamic equations of state without the explicit use of underlying microscopic models. There is nothing resembling the summation over microstates to find a partition function. A hope is that the geometric theory can reveal universal properties, independent of microscopic details and common to broad classes of systems. In addition, the geometric theory yields results even in cases where the sum for the partition function for corresponding cases is known to diverge, such as the self-gravitating gas. Figure 1 contrasts the philosophies of the geometric theory and statistical mechanics.

Since the subject of thermodynamic curvature was reviewed [3], a number of papers on this topic have been published. Here is a representative sample: Refs. [6–15].

This paper is laid out as follows. First, I summarize the Riemannian geometric theory of thermodynamics (hereafter referred to as the geometric theory). Second, I present the statistical mechanics of the power-law interacting gas and show how it simplifies the geometric theory. Third, I present general theorems for this problem. Fourth, I discuss methods of numerical computation. Fifth, I discuss how the geometric theory can accommodate first-order phase transitions. Sixth, I discuss several special cases of this theory for repulsive interactions. Finally, I make some brief remarks about attractive interactions.

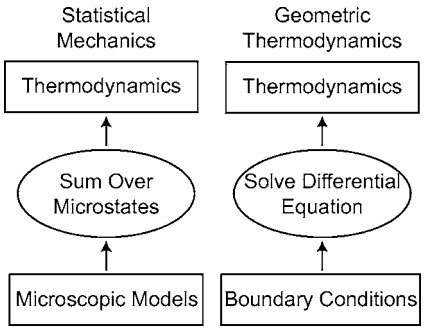

FIG. 1. Contrasting philosophies of statistical mechanics and the geometric theory. For microscopic models we substitute boundary conditions and/or simplifying mathematical forms for the equations of state. (These may, of course, reflect microscopic conditions.) Instead of computing a partition function, we solve a differential equation for the thermodynamics.

II. GEOMETRIC THEORY

Although the geometric theory is more general [3,16], I restrict discussion to a three-dimensional pure fluid in temperature, density coordinates. The thermodynamic notation in this paper follows that of Ref. [3].

Consider an open subsystem A_V, with fixed volume V, of an infinite pure fluid system A_{V_0}. A_V has fluctuating temperature and number density (T,ρ). A_{V_0} has volume V_0 (tending to infinity) and fixed temperature and number density (T_0,ρ_0). The classical thermodynamic fluctuation theory [17] asserts that the probability of finding the thermodynamic state of A_V in a small rectangle in thermodynamic state space with bounding coordinates (T,ρ) and $(T+dT,\rho+d\rho)$ is

$$P_V(T,\rho)dT\,d\rho = C\exp\left(\frac{S_{total}}{k_B}\right)dT\,d\rho, \tag{1}$$

where S_{total} is the entropy of A_{V_0} when its subsystem A_V is in the state (T,ρ), k_B is Boltzmann's constant, and C is a normalization factor.

The total entropy S_{total} is maximized in the equilibrium state $(T,\rho)=(T_0,\rho_0)$. Expanding S_{total} to second order about this maximum yields the Gaussian approximation to the thermodynamic fluctuation theory:

$$P_V(T,\rho)dT\,d\rho = \left(\frac{V}{2\pi}\right)\exp\left(-\frac{V}{2}[g_{TT}(\Delta T)^2 + g_{\rho\rho}(\Delta\rho)^2]\right)\sqrt{g}\,dT\,d\rho, \tag{2}$$

where $\Delta T=T-T_0$, $\Delta\rho=\rho-\rho_0$,

$$g_{TT} = \frac{1}{k_B T^2 V}\left(\frac{\partial U}{\partial T}\right)_\rho, \tag{3}$$

$$g_{\rho\rho} = \frac{1}{k_B T\rho}\left(\frac{\partial p}{\partial \rho}\right)_T, \tag{4}$$

and

$$g = g_{TT}g_{\rho\rho}. \tag{5}$$

Here, U is the internal energy and p is the pressure. This Gaussian approximation is valid for large V [18].

The quadratic form

$$(\Delta l)^2 = g_{TT}(\Delta T)^2 + g_{\rho\rho}(\Delta\rho)^2 \tag{6}$$

constitutes a positive-definite Riemannian metric on the two-dimensional thermodynamic state space of points with coordinates (T,ρ) [2,3]. Physically, the interpretation for distance between two thermodynamic states is clear from Eq. (2): *the less probable a fluctuation between two states, the further apart they are*. The thermodynamic metric serves as the foundation for a thermodynamic fluctuation theory which extends the classical thermodynamic fluctuation theory Eq. (1) beyond the Gaussian approximation in a covariant and consistent way [19–21]. I add that such probability metrics are familiar in the broader context of information theory [3,22–24].

Central to any Riemannian geometry is the Riemannian curvature scalar R, which follows naturally from the metric [25]. The value of R for any particular thermodynamic state is independent of which coordinate system is used to label the states [26]. Hence, R is a property of the "true" physics and lays claim on these grounds alone as being an important object of study.

Ruppeiner [2] found that R is zero for all states of the pure ideal gas, suggesting that R is a measure of interactions. R was also found to have units of volume (e.g., meters cubed) and to diverge to infinity at the critical point of a pure fluid in the same way as the correlation volume. It was naturally hypothesized that [2]

$$R = \kappa_2\xi^3, \tag{7}$$

where ξ is the correlation length and κ_2 is a dimensionless constant with absolute value of order unity. This idea has been verified in a number of cases with known thermodynamics and correlation length [3] and has been amplified by the finding that R marks the volume where the Gaussian thermodynamic fluctuation theory Eq. (2) breaks down regardless of coordinates [20].

To make the connection between the correlation volume and the free energy, invoke the hypothesis of hyperscaling in the theory of critical phenomena [27]. It asserts that near the critical point the "singular part" of the free energy per volume

$$\phi = \frac{p}{T} = s - \frac{u}{T} + \frac{\mu\rho}{T} \tag{8}$$

is inversely proportional to the correlation volume:

$$(\phi)_{singular} = -\frac{\kappa_1 k_B}{\xi^3}, \tag{9}$$

where κ_1 is a dimensionless constant with absolute value of order unity, S is the entropy, $s=S/V$ is the entropy per volume, $u=U/V$ is the internal energy per volume, and μ is the chemical potential.

Combining Eqs. (7) and (9) yields

$$R = -\kappa\left(\frac{k_B}{\phi}\right)_{singular}, \tag{10}$$

where

$$\kappa = \kappa_1\kappa_2. \tag{11}$$

In words, this geometric equation states that *the curvature is inversely proportional to the inverse of the free energy density*. The somewhat loose argument presented for it here assumes that we are near the pure fluid critical point where ξ^3 is large. However, the viewpoint in this paper is to regard Eq. (10) as a general postulate in its own right, to be explored in as many situations as possible. Particularly interesting in this regard is the demonstration by Kaviani and Dalafi-Rezaie [13] that the free energy density of the classical ideal paramagnetic gas, free of any interactions, satisfies the geometric equation (10) exactly.

Somewhat vague at this point is precisely what is meant by the "singular part" of the free energy. Clearly, it is to be

formed from the free energy ϕ or its inverse by subtracting the portion not connected with organized fluctuations, curvature, or interactions. While this may sound arbitrary, in practice assumptions about analyticity usually leave us little choice about the appropriate subtraction. Likewise, analyticity assumptions yield the value for κ.

The equation for the curvature scalar in (T,ρ) coordinates is [28]

$$R = \frac{1}{\sqrt{g}}\left[\frac{\partial}{\partial T}\left(\frac{1}{\sqrt{g}}\frac{\partial g_{\rho\rho}}{\partial T}\right) + \frac{\partial}{\partial \rho}\left(\frac{1}{\sqrt{g}}\frac{\partial g_{TT}}{\partial \rho}\right)\right]. \tag{12}$$

Since, by the rules of thermodynamics, all thermodynamic quantities may be expressed in terms of ϕ and its derivatives, the geometric equation (10) may be expressed as a partial differential equation for ϕ. We will see below how this equation manifests itself in the case of power-law interactions.

III. POWER-LAW INTERACTIONS

Near the critical point, a generalized homogenous function was used to simplify the solution process [4,16]. Here, I start with the integral equations of state in the context of power-law interactions. Although the statistical mechanical calculation stalls in the attempt to compute the partition function, it does produce a formalism which, with the geometric theory, results in an ordinary differential equation yielding the full thermodynamics.

A. Statistical mechanics

Define the radial distribution function $g(r,T,\rho)$ as follows [29,30]. Consider an atom at the origin and ask for the average number of atoms contained in a thin spherical shell centered at the origin, with inner radius r and outer radius $r+dr$. By definition, this is

$$\rho g(r,T,\rho) 4\pi r^2\, dr. \tag{13}$$

At large r, atoms are randomly arranged with respect to the origin and $g(r,T,\rho)$ is unity. At smaller r interactions play a role and $g(r,T,\rho)$ generally deviates from unity. By virtue of its definition, $g(r,T,\rho)$ is never negative.

Elementary arguments in statistical mechanics [29] show that the internal energy may be written as

$$\frac{U}{Nk_BT} = \frac{3}{2} + \frac{\rho}{2k_BT}\int_{r=0}^{\infty} u(r) g(r,T,\rho) 4\pi r^2\, dr, \tag{14}$$

where $u(r)$ is the potential energy between two atoms separated by a distance r and $N=\rho V$ is the particle number. Likewise, the pressure is

$$\frac{pV}{Nk_BT} = 1 - \frac{\rho}{6k_BT}\int_{r=0}^{\infty} r\frac{du(r)}{dr} g(r,T,\rho) 4\pi r^2\, dr. \tag{15}$$

These two integral equations of state are generally valid for any interacting monatomic pure gas, so long as the integrals converge. However, their practical use is limited because $g(r,T,\rho)$ is not, *a priori*, known. My method around this difficulty is to consider the case where $u(r)$ satisfies the differential equation

$$r\frac{du(r)}{dr} = -\alpha u(r), \tag{16}$$

where α is the exponent in the power-law solution. Here, the integrals in Eqs. (14) and (15) become proportional to one another, and, as I will demonstrate in the next subsection, the geometric theory will allow us to write them as the solution to an ordinary differential equation.

The unique solution to Eq. (16) is a power-law interaction potential energy:

$$u(r) = \frac{\gamma}{r^{\alpha}}, \tag{17}$$

where γ is a constant giving the strength of the interaction. This form allows us to write Eqs. (14) and (15) as

$$U = \frac{3}{2}Nk_BT[1 - ab(T,\rho)] \tag{18}$$

and

$$p = \rho k_BT[1 - b(T,\rho)], \tag{19}$$

where

$$b(T,\rho) = -\frac{\rho}{6k_BT}\gamma\alpha\int_{r=0}^{\infty} r^{-\alpha} g(r,T,\rho) 4\pi r^2\, dr \tag{20}$$

and

$$a = \frac{2}{\alpha}. \tag{21}$$

I restrict attention to $a \geqslant 0$ since interactions with the absolute value of the potential energy growing with distance are unphysical.

For attractive interactions ($\gamma<0$) convergence at the upper integral limit in Eq. (20) certainly requires $\alpha>3$. However, with $\alpha>3$, the integral diverges at the lower limit, since attractive interactions would lead one to expect $g(r,T,\rho)$ to exceed unity for small r. Statistical mechanics offers then no case where the integral equations of state converge for $\gamma<0$. Interesting alternative thermodynamics, without traditional thermodynamic limits, have been reported [32,33]. For the viewpoint in this paper, see Sec. VIII.

For repulsive interactions ($\gamma>0$), convergence at the upper integral limit in Eq. (20) requires again $\alpha>3$. But for $\alpha>3$ we are saved from the divergence at the lower limit by a vanishing $g(r,T,\rho)$. This is known indirectly from rigorous statistical mechanics [34] which indicates that a thermodynamic limit will exist for continuum systems in three dimensions provided that the potential is both "tempered" and "stable." For repulsive interactions with $\alpha>3$ the potential satisfies both these conditions. This is significant, since it offers a situation where the geometric theory may be directly compared with statistical mechanics.

It is straightforward to show that the Maxwell relation

$$\left(\frac{\partial p}{\partial T}\right)_{V,N} = \left(\frac{\partial S}{\partial V}\right)_{T,N} \tag{22}$$

is satisfied if and only if

$$b(T,\rho) = b(x), \tag{23}$$

where

$$x = \frac{\rho}{T^{3a/2}}. \tag{24}$$

This leads, finally, to

$$U = \frac{3}{2}Nk_BT[1 - ab(x)] \tag{25}$$

and

$$p = \rho k_BT[1 - b(x)]. \tag{26}$$

My notation is based on that in applications to self-gravitating systems [5,35]. These expressions lead to great simplicity, since a single isotherm, isochore, or isobar is sufficient to determine the entire phase diagram. Since it makes little difference, I will usually work with isotherms.

Statistical mechanics takes us little further at this point, since we cannot do the integral for $b(x)$. But, in the next subsection we will see how the geometric theory allows us to express $b(x)$ as the solution to a differential equation.

B. Geometric theory

I now express the geometric equation as an ordinary differential equation. Substituting Eqs. (25) and (26) into Eqs. (3) and (4) for the metric elements yields

$$g_{TT} = \frac{3\rho}{4T^2}[2 - 2ab(x) + 3a^2xb'(x)] \tag{27}$$

and

$$g_{\rho\rho} = \frac{[1 - b(x) - xb'(x)]}{\rho}. \tag{28}$$

Substituting these equations into Eq. (12) for the curvature yields

$$RT^{3a/2} = n_1/d_1, \tag{29}$$

where

$$\begin{aligned} n_1 = {} & 4b'(x) - 6ab'(x) - 3a^2b'(x) - 2ab(x)b'(x) + 9a^2b(x)b'(x) + 3a^3b(x)b'(x) - 2a^2b(x)^2b'(x) - 3a^3b(x)^2b'(x) + 2axb'(x)^2 \\ & + 7a^2xb'(x)^2 - 9a^3xb'(x)^2 + 2a^2x^2b'(x)^3 + 3a^3x^2b'(x)^3 + 2xb''(x) - 4axb''(x) - 3a^2xb''(x) + 7a^2xb(x)b''(x) + 3a^3xb(x)b''(x) \\ & - 2a^2xb(x)^2b''(x) - 3a^3xb(x)^2b''(x) + 2ax^2b'(x)b''(x) + 6a^2x^2b'(x)b''(x) - 3a^3x^2b'(x)b''(x) - 2a^2x^2b(x)b'(x)b''(x) \\ & - 3a^3x^2b(x)b'(x)b''(x) \end{aligned} \tag{30}$$

and

$$d_1 = [-1 + b(x) + xb'(x)]^2[2 - 2ab(x) + 3a^2xb'(x)]^2. \tag{31}$$

Remarkably, terms in the third derivatives of $b(x)$ and terms nonlinear in $b''(x)$ cancel in the calculation.

It is now possible to determine the "singular part" of the free energy. Assume that $b(x)$ is analytic at $x=0$ and expand

$$b(x) = \sum_{i=1}^{\infty} b_i x^i = b_1x + b_2x^2 + b_3x^3 + O(x^4), \tag{32}$$

where the b_i's are constant coefficients. The leading coefficient $b_0=0$ since Eqs. (25) and (26) must reduce to the ideal gas expression as $x \to 0$. Substituting this series into Eq. (29) for the curvature yields the series

$$\begin{aligned} RT^{3a/2} = {} & -\frac{1}{4}(-4 + 6a + 3a^2)b_1 + \frac{1}{4}[(16 - 16a - 20a^2 + 6a^3 \\ & + 9a^4)b_1^2 - 4(-3 + 5a + 3a^2)b_2]x + O(x^2). \end{aligned} \tag{33}$$

We likewise find with Eq. (26) that

$$\frac{k_BT}{p}T^{3a/2} = \frac{1}{x} + b_1 + (b_1^2 + b_2)x + O(x^2). \tag{34}$$

The geometric equation (10) would have us set these two series proportional to each other. But this fails because of the $1/x$ term in Eq. (34). This term reflects the ideal gas contribution to the inverse of the free energy and has nothing to do with either interactions or curvature. Hence, I subtract it as the "nonsingular" part and set

$$\left(\frac{k_B}{\phi}\right)_{singular} = \left(\frac{k_BT}{p} - \frac{1}{\rho}\right). \tag{35}$$

The corresponding series is

$$\left(\frac{k_B}{\phi}\right)_{singular} T^{3a/2} = b_1 + (b_1^2 + b_2)x + O(x^2). \tag{36}$$

Substituting the series Eqs. (33) and (36) into Eq. (10) yields

$$\kappa = \frac{1}{4}(-4 + 6a + 3a^2). \tag{37}$$

It also shows that b_1 is a free constant in the theory from which all of the other b_i's follow uniquely by a series solution method. Clearly, $\kappa=0$ for $a=-2.5275$ and 0.5275. The unphysical negative value is not considered here, but the positive value will be discussed in Sec. VIII.

The units of b_1 are such as to make the product $b_1 x$ dimensionless. From Eq. (20), systems with attractive interactions ($\gamma<0$ and $\alpha>0$) are expected to have $b(x)>0$ for all x, and hence $b_1>0$. For systems with repulsive interactions ($\gamma>0$ and $\alpha>0$), we expect the opposite sign.

I conclude this subsection by displaying the geometric equation in the form solved here. By substituting Eqs. (29) and (35) into Eq. (10) [p is evaluated with Eq. (26)], changing variables, and rearranging, the geometric equation becomes two coupled first-order differential equations:

$$\frac{db}{dt} = w \tag{38}$$

and

$$\frac{dw}{dt} = h(b,w), \tag{39}$$

where

$$t = \ln(|b_1|x) \tag{40}$$

and

$$h(b,w) = n_2/d_2, \tag{41}$$

with

$$n_2 = -(-16b + \cdots + 27a^6 b w^4) \tag{42}$$

a polynomial of 75 terms, each a product of powers of a, b, and w, and

$$d_2 = 4(-1+b)(-2+4a+3a^2-7a^2b-3a^3b+2a^2b^2+3a^3b^2 - 2aw-6a^2w+3a^3w+2a^2bw+3a^3bw). \tag{43}$$

The geometric equation in this form becomes the basis for the theorems and numerical solutions below.

IV. THEOREMS

In this section, I present several theorems for statistical mechanics and the geometric theory.

A. Statistical mechanics

To simplify the language, introduce the phrase "scaling transformation" for the multiplication by factors,

$$(r,T,\rho,\gamma) \to (\lambda^{1/\alpha}r, \epsilon T, \lambda^{-3/\alpha}\rho, (\lambda\epsilon)\gamma), \tag{44}$$

where λ and ϵ are dimensionless constants, and for calculating with the rescaled values of (r,T,ρ,γ). It is straightforward to prove [36] the following.

Theorem 1: *Under a scaling transformation, the radial distribution function is unchanged*,

$$g(\lambda^{1/\alpha}r, \epsilon T, \lambda^{-3/\alpha}\rho) = g(r,T,\rho). \tag{45}$$

Theorem 1 and Eq. (20) allow an immediate proof of the following.

Theorem 2: *Under a scaling transformation, the function* $b(T,\rho)$ *is unchanged*:

$$b(\epsilon T, \lambda^{-3/\alpha}\rho) = b(T,\rho). \tag{46}$$

From this follows our main scaling theorem,

Theorem 3: *Under a scaling transformation, the function* $b(x)$ *is unchanged*:

$$b((\lambda\epsilon)^{-3/\alpha}x) = b(x). \tag{47}$$

For a given α, the thermodynamics is thus given by a single function $b(x)$ and a single scaling factor reflecting the interaction strength.

The next statistical mechanical theorem concerns high-density states of systems with repulsive interactions, $\gamma>0$. As we compress at fixed T, the atoms are intuitively expected to lock increasingly into place with one another in a lattice where most of the energy is potential, and with very little vibration. This has been verified by computer simulations [37], where the lattice was found to be fcc [38]. A quantum mechanical example is the Wigner lattice [39].

The assumption of a lattice limit at fixed T, $\gamma>0$, and $x\to\infty$ leads to the following.

Theorem 4: *In the lattice limit*,

$$b(x) \to -\gamma\left(\frac{G}{3k_B a}\right)x^{2/3a}, \tag{48}$$

where

$$G = \sum_{i=2}^{N}\left(\frac{r_0}{r_i}\right)^{\alpha} \tag{49}$$

is a structure constant independent of ρ *and* T, $r_0=\rho^{-1/3}$, *and* r_i *is the distance between the i'th atom and the origin, assumed to correspond to the position of the first atom.*

For proof, note that as the density increases, the potential energy grows without limit, while the kinetic energy stays fixed at $\frac{3}{2}Nk_BT$. By Eq. (25) then, $-b(x)$ must get large, and a straightforward calculation of the potential energy now establishes the theorem. With this theorem we see that in the lattice limit, the pressure depends only on the density:

$$p \sim \rho^{(\alpha+3)/3}. \tag{50}$$

From Theorem 4 and Eq. (28), we obtain the following.

Theorem 5: *In the lattice limit*,

$$\rho g_{\rho\rho} \to \gamma\left(\frac{G}{3k_B a}\right)\left(\frac{3a+2}{3a}\right)x^{2/3a}. \tag{51}$$

This is positive for all $a>0$, as it must be, and approaches infinity as $x\to\infty$, corresponding to an incompressible limiting lattice.

The next theorem assumes the Dulong-Petit law in the lattice limit,

$$\left(\frac{\partial U}{\partial T}\right)_{\rho} \to 3Nk_B. \tag{52}$$

Equation (3) leads with this to the next theorem.

Theorem 6: *In the lattice limit*,

$$\frac{T^2}{\rho} g_{TT} \to 3. \tag{53}$$

To compare the geometric theory with statistical mechanics in Sec. VII, we must connect the free thermodynamic constant b_1 with the interatomic potential strength γ. The low-density virial expansion [29]

$$\frac{p}{\rho k_B T} = 1 + B_2\rho + B_3\rho^2 + O(\rho^3), \tag{54}$$

where the B_n's are the temperature dependent virial coefficients, lets us do this. Statistical mechanics [29] yields

$$B_2 = -\frac{1}{2}\int_{r=0}^{\infty}\left[\exp\left(-\frac{u(r)}{k_B T}\right) - 1\right] 4\pi r^2\, dr. \tag{55}$$

Comparing with Eq. (32) from the thermodynamic method leads to the following theorem.

Theorem 7:

$$b_1 = -\frac{2\pi}{\alpha}\left(\frac{\gamma}{k_B}\right)^{3/\alpha}\int_{z=0}^{\infty}[1-\exp(-z)]z^{-(3/\alpha)-1}\, dz. \tag{56}$$

This integral converges if and only if $\alpha > 3$.

B. Geometric theory

The pair of differential equations (38) and (39) are autonomous [40] since the right-hand sides do not depend explicitly on t. They are thus invariant with respect to an additive constant for t, or, equivalently, a multiplicative factor for $x: x \to \lambda x$. Furthermore, the solution follows uniquely on giving two constants b_0 and b_1. Since $b_0 = 0$ is common to all our solutions, at least for small x, b_1 (proportional to λ) is the only free factor, proving the following.

Theorem 1′: *If $b(x)$ is a solution to the geometric equation, then so is $b(\lambda x)$, and all solutions starting at the origin are given by a single function $b(x)$ and a single scaling factor, proportional to b_1.*

This scaling and universality of solutions is consistent with Theorem 3.

The remaining theorems concern lattice limiting solutions.

Theorem 2′: *For any a different from zero, and for any constant k and all x, the simple expression*

$$b(x) = kx^{2/3a} + \frac{1}{a} \tag{57}$$

is an exact solution to Eqs. (38) and (39).

The proof of this remarkable theorem is by direct calculation.

This expression yields an exact relation between b and w:

$$w = \frac{2}{3a}b - \frac{2}{3a^2}, \tag{58}$$

independent of k.

The form in Theorem 2′ has the same limiting x dependence as that in Theorem 4. Despite this, however, the significance of Theorem 2′ is not transparent. I offer no proof that solutions starting at the origin *must* approach this form. But, in Sec. VII, I show numerically that a significant class of solutions does approach this form asymptotically, establishing a limiting correspondence with statistical mechanics.

Here are some observations about the metric elements in the lattice limit. The form in Theorem 2′ implies $\rho g_{\rho\rho}$ has the same x dependence as that in Theorem 5. But, Theorem 2′ has $g_{TT} = 0$ for all x, not what we want physically from the Dulong-Petit Theorem 6. Perhaps a more accurate limiting form for $b(x)$ remains to be found.

Finally, Eqs. (10), (26), and (35) yield the last theorem.

Theorem 3′: *For any function $b(x)$ with $|b(x)| \to \infty$, the curvature goes to*

$$R \to \frac{\kappa}{\rho}. \tag{59}$$

This lattice limiting form has the curvature approaching the order of the volume per atom. Small curvature at high density is similar to the result found earlier in the Takahashi gas [31].

V. NUMERICAL SOLUTION METHODS

The study of specific cases requires full numerical solutions of the geometric equation. First, note that since the differential equations (38) and (39) are autonomous, the solution curves in (b,w) space are independent of $|b_1|$. Mathematically, a solution curve may be started from any nonsingular point (b,w). But, I start all our solution curves from the ideal gas point $(b,w) = (0,0)$ with $x = 0$, reasoning that if there are any stable physical states, this would be one.

Solution curves could conceivably encounter a variety of singular points. At singular points either both sides of Eqs. (38) and (39) are zero, or $h(b,w)$ diverges. Singular points come in five types: (1) points off the b axis where the denominator of $h(b,w)$ is zero, but its numerator is not zero; (2) points off the b axis where the numerator and the denominator of $h(b,w)$ are both zero; (3) points on the b axis where the numerator of $h(b,w)$ is zero, but its denominator is not zero; (4) points on the b axis where the denominator of $h(b,w)$ is zero, but its numerator is not zero, and (5) points on the b axis where both the numerator and the denominator of $h(b,w)$ are zero.

Generally, type 1 singular points are located along curves in (b,w) space. The other types are isolated points. For type 2 singular points, we typically get cancelling zeros along approaching solution curves, which allows us to, in effect, treat $h(b,w)$ as analytic there. Such "crossing points" were important in Ref. [4], but we will not see an example here.

Type 1 singular curves are readily classified. From Eq. (43), we see that d_2, the denominator of $h(b,w)$, is zero for

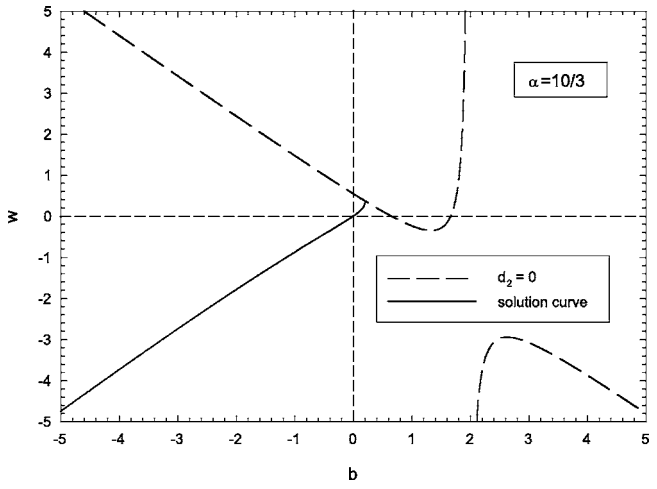

FIG. 2. Type 1 singular curve where $d_2=0$ [in Eq. (43)] for $a=3/5$. This figure is representative of other values of a and shows the curve going to $\pm\infty$ in the second and fourth quadrants with slope -1. It also reaches $\pm\infty$ at $b_c=1.9825$. Also shown is the solution curve for both positive and negative b_1. The curve goes to infinity analytically in the third quadrant in accord with the x dependence in Theorem 4. It encounters the type 1 singular curve in the first quadrant.

all a if $b=1$. But, a zero with $b>0$ holds no interest for repulsive interactions, and we consider it no further. Otherwise, for every a and b, there is exactly one value of w corresponding to $d_2=0$, and for every a and w, there are either two or no real values of b corresponding to $d_2=0$. Type 1 singular curves go asymptotical to infinity in the second and fourth quadrants since for any nonzero a, $w/b\to -1$ as $b\to\pm\infty$.

For every nonzero a (except $a=1$), there is exactly one finite critical value $b=b_c$ where $w\to\pm\infty$ on the type 1 singular curve:

$$b_c=\frac{2+6a-3a^2}{2a+3a^2}. \tag{60}$$

This value separates the type 1 singular curve into two branches. As $a\to 0$, $b_c\to\infty$, and as $a\to\infty$, $b_c\to -1$. Since for $a=2.2910$, $b_c=0$, all the type 1 singular curves with $0<a<2/3$ correspond to the left branch. Figure 2 shows these branches for $a=3/5$, where $b_c=1.9825$. The qualitative shape of the type 1 singular curves is the same for all $a>0$.

From Eq. (41), we can show that the ideal gas point (0,0) is a type 3 singular point for all values of a except $a=-1.7208$ and 0.3874, which are type 5's. (The negative value does not concern us here, but the positive value comes up again in Sec. VI.) The standard approach to a type 3 singular point starts by linearizing the differential equations (38) and (39) about that point. Very near the origin

$$\frac{db}{dt}=w \tag{61}$$

and

$$\frac{dw}{dt}=a_1 b+a_2 w, \tag{62}$$

where a_1 and a_2 are constants:

$$a_1=\frac{-4+6a+3a^2}{-2+4a+3a^2} \tag{63}$$

and

$$a_2=\frac{2-2a}{-2+4a+3a^2}. \tag{64}$$

Trying a solution of the form

$$b=re^{\lambda t} \tag{65}$$

and

$$w=se^{\lambda t}, \tag{66}$$

where λ, r, and s are constants, leads to a characteristic equation for λ:

$$\lambda^2-a_2\lambda-a_1=0, \tag{67}$$

as a necessary condition for nonzero solutions for r and s. The roots are

$$\lambda=1 \quad \text{or} \quad \lambda=\frac{4-6a-3a^2}{-2+4a+3a^2}. \tag{68}$$

The former possibility yields

$$b(x)=rx, \tag{69}$$

consistent with the first term in the series Eq. (32).

Since (0, 0) is a singular point, I start numerical solutions at slightly removed from it using the series Eq. (32) to generate initial conditions. Solution curves with attractive interactions ($b_1>0$) move into the first quadrant and those with repulsive interactions ($b_1<0$) into the third quadrant. With increasing t, solution curves propagate until they either drift off to infinity or encounter some singular point or curve.

VI. FIRST-ORDER PHASE TRANSITIONS

Repulsive power-law interacting systems are known to offer a simple model for melting/freezing transitions [41]. Computer simulations [37] have revealed such phase transitions for $\alpha=4$, 6, 9, and 12. Consider compressing a system at constant T starting at the ideal gas (0, 0), as in Fig. 3. Initially, the fluid curve is traversed. But, in computer studies [37], this curve eventually terminates at some state A, and there is a jump to a state B which shows solid fcc ordering. At higher densities, this solid curve is expected to increasingly take on the limiting lattice functional form in Eq. (48).

For a first-order phase transition we require $\Delta T=0$ and $\Delta p=0$, but discontinuous energy and entropy, corresponding to a latent heat:

$$T\Delta S=\Delta U+p\Delta V. \tag{70}$$

Here $\Delta S=S_B-S_A$, etc., where the subscripts refer to states A and B. The conditions $\Delta T=0$ and $\Delta p=0$ yield, with Eq. (26),

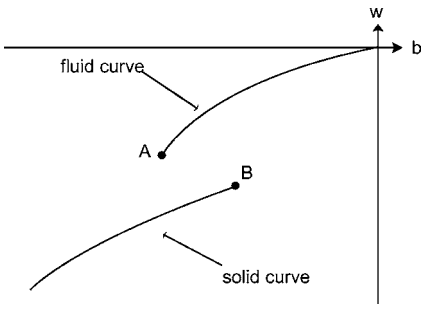

FIG. 3. Fluid and solid curves in (b,w) space. The fluid curve starts at the ideal gas state (0,0). The solid curve is picked to approach the asymptotic lattice state Eq. (48) at increasing density and constant T. Computer simulations reveal that as we compress the fluid, the Gibbs free energy will eventually lower itself by jumping from a fluid state A to a solid state B.

$$x_A(1-b_A)=x_B(1-b_B). \tag{71}$$

If we know $b(x)$ for both fluid and solid curves, then this constant pressure relation yields x_B from x_A. It is expected that $-b_1x_A$, $-b_1x_B$, b_A, and b_B depend only on the exponent α, and not on the interaction strength γ [37].

This freezing transition results from the atoms abruptly lowering their Gibbs free energy by arranging themselves into a more ordered structure. Since the geometric theory knows nothing, *a priori*, about solid structures, it is unlikely to predict such a phase transition by itself. But, we may easily include one. Start with fluid and solid curves solving the geometric equation. These should go to the appropriate low and high density limits. Then pick a transition point (x_A,b_A) on the fluid curve. The constant pressure relation then gives (x_B,b_B), and the full thermodynamics is determined.

Since the entropies of both the fluid and the solid curves contain an undetermined constant, which the geometric theory does not relate to each other, the state A cannot be determined from the geometric theory alone. There is nothing like a Maxwell equal area construction because there is generally no solution curve (however unphysical) connecting the points A and B. Nevertheless, the geometric theory does allow us to include a first-order phase transition, if it is needed.

VII. EXAMPLES

In this section I look at specific cases with various values of a, all having repulsive interactions, $b_1<0$. I summarize the previous statistical mechanical findings regarding thermodynamic limits in Fig. 4. Repulsive interactions offer a regime where the thermodynamic limit exists: $0<a<2/3$. With no loss of generality, set $k_B=\gamma=1$. In these units, both b_1 and x are dimensionless.

A. Repulsive potential energy $u(r)=\gamma r^{-10/3}$

Here, $a=3/5$ and $\kappa=17/100$. This a value falls into the regime labeled "convergent, $\kappa>0$" in Fig. 4, where all solutions I tried drift off analytically to infinity in the third quadrant of (b,w) space with the same x dependence as that in Theorem 4.

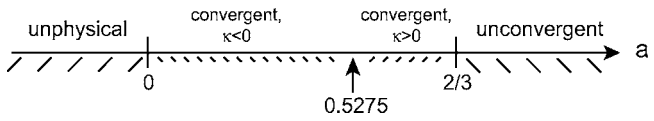

FIG. 4. The statistical mechanical regimes for various values of a. Since no case with attractive interactions has a thermodynamic limit, our terminology is directed at cases with repulsive interactions. The "unphysical" regime $a<0$ corresponds to interaction potentials growing with distance. The "unconvergent" regime $a\geqslant 2/3$ has the integral in Eq. (20) diverging at the upper limit. The "convergent" regime $0<a<2/3$ corresponds to a converging integral in Eq. (20). The value $a=0.5275$ reflects a changing sign of κ, where the thermodynamic solutions change character.

The origin (0, 0) for $a=3/5$ is a type 3 singularity. There are no singularities in the third quadrant or on the negative b axis. Figure 2 shows a full solution curve. Of particular interest is the limiting case for $b_1<0$ and large x. Figure 5 shows $-b(x)/(-b_1x)^{10/9}$ as a function of $-b_1x$. As x increases, this quantity approaches a constant limit, as physically expected from Theorem 4.

To compare this constant with that in Theorem 4, we must relate γ and b_1 using the virial theorem expression in Theorem 7. For $k_B=\gamma=1$, Eq. (56) yields $b_1=-19.925$. With the limiting value in Fig. 5, we get

$$b(x)\to -11.00x^{10/9}. \tag{72}$$

In statistical mechanics, the numerical computation of the structure constant G in Eq. (49) for the fcc lattice yields

$$b(x)\to -22.87x^{10/9}. \tag{73}$$

The coefficients in the two approaches are within a factor of about 2, reasonable agreement given that the thermodynamics has nothing built into it about atomic structure.

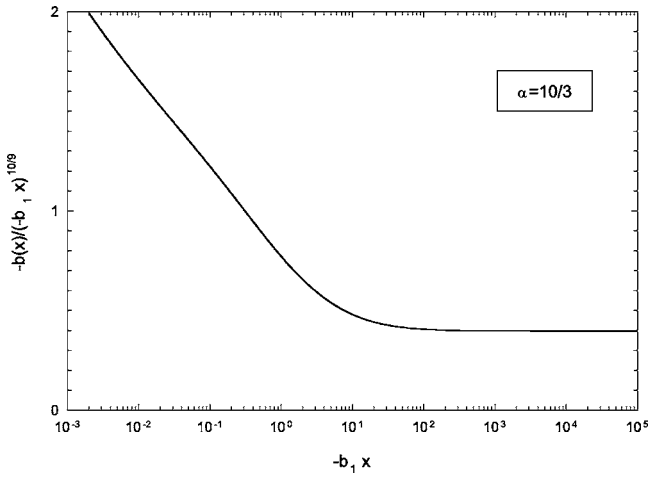

FIG. 5. The function $-b(x)/(-b_1x)^{10/9}$ versus $-b_1x$ for $a=3/5$. For large x, the curve approaches a constant value of 0.3958. The approach to a constant limit for large x is physically expected from Theorem 4.

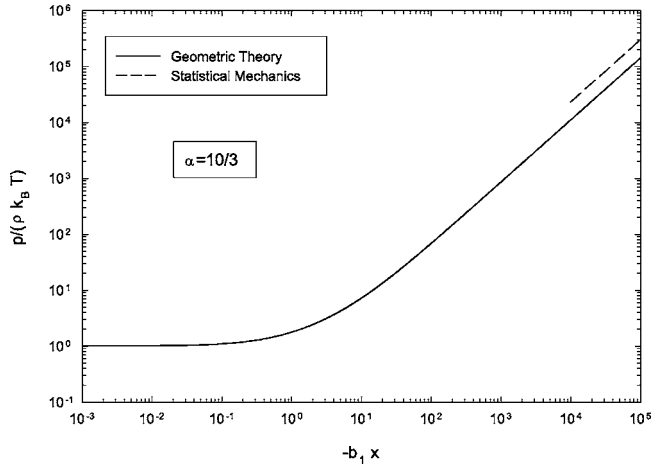

FIG. 6. $p/(\rho k_B T)$ as a function of $-b_1 x$ for $a=3/5$. For small x the curve has the constant ideal gas value 1. As x increases, there is a transition to the diverging limiting form in Theorem 4. The dashed line shows the limiting behavior from statistical mechanics in Eq. (73) assuming an fcc lattice.

Figure 6 shows $p/(\rho k_B T)$ vs. $-b_1 x$ calculated with the geometric theory. This curve relating dimensionless quantities is universal, independent of the value of $|b_1|$. It starts with the constant ideal gas value of 1, and, as the gas is compressed, makes a transition to the x dependence in Theorem 4. Also shown is the limiting form from statistical mechanics calculated with Eq. (73). The calculation of the full curve with statistical mechanics is not feasible.

Turn now to universal curves for the metric elements. Figure 7 shows $T^2 g_{TT}/\rho$ as a function of $-b_1 x$ for the geometric theory. At small x, the curve starts with its ideal gas value 3/2, and then increases monotonically with x to a finite limit 2.9412. Also shown is the Dulong-Petit limit of 3. Figure 8 shows $\rho g_{\rho\rho}$ as a function of $-b_1 x$ for the geometric theory. At small x, the curve starts with its ideal gas value 1, and then increases without limit following the x dependence in Theorem 5. The limiting statistical mechanical expression Eq. (51) is also shown.

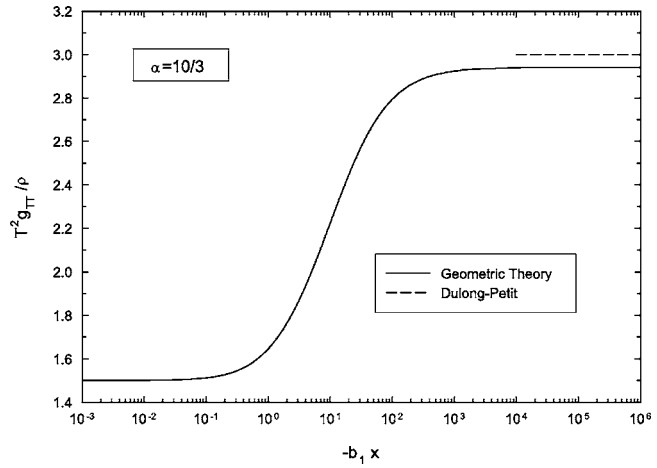

FIG. 7. $T^2 g_{TT}/\rho$ as a function of $-b_1 x$ for the geometric theory with $a=3/5$. As x increases, the curve rises from its ideal gas value 3/2 to a limiting value 2.9412.

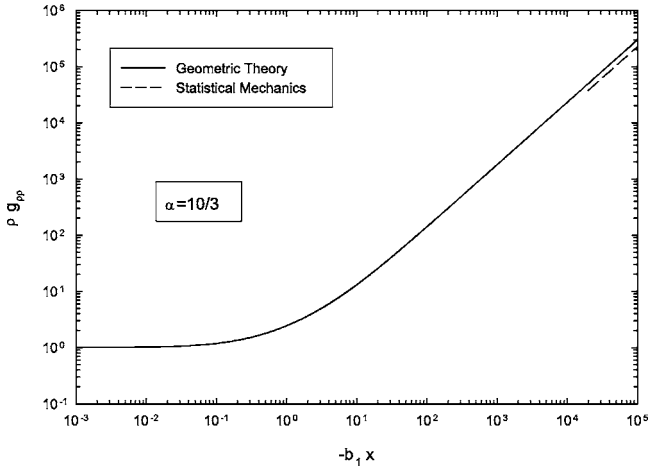

FIG. 8. $\rho g_{\rho\rho}$ as a function of $-b_1 x$ for the geometric theory with $a=3/5$. As x increases, the curve rises monotonically from its ideal gas value of 1 to infinity following the x dependence in Theorem 5, which is also shown.

To assess other values of a in the "convergent, $\kappa>0$" regime, I did numerical solutions of the geometric equation for a number of a's and found them all qualitatively similar to the one for $a=3/5$ above. None of the solutions have singularities either in the third quadrant or on the negative b axis. The solution curves all went analytically from (0, 0) to infinity in the third quadrant with the same x dependence as that in Theorem 4. Figure 9 shows the limit of $-b(x)/(-b_1 x)^{2/3a}$ as $x\to\infty$ as a function of a. This limit decreases to zero as a decreases to 0.5275, where κ becomes zero as it changes sign. For smaller values of a, where κ is negative, the behavior of the solution curves is quite different, as will be discussed in the next subsection.

Figure 10 shows the limiting values of $T^2 g_{TT}/\rho$ as $x\to\infty$ computed numerically with the geometric equation for a range of a values in the "convergent, $\kappa>0$" regime. Values are all positive, as required by thermodynamic stability, and diverge as a decreases to 0.5275. For reasons not understood,

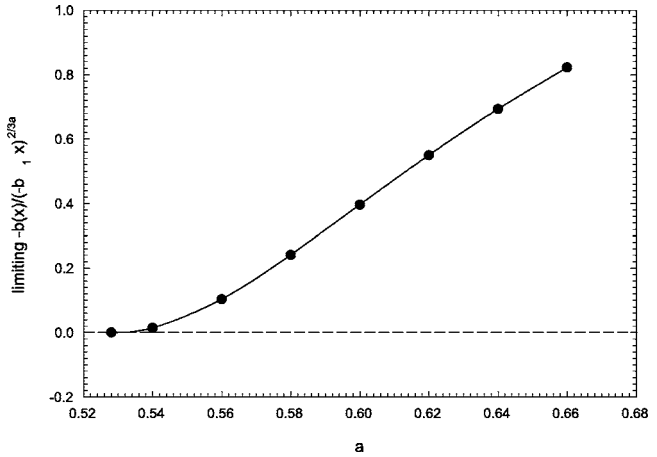

FIG. 9. Limiting values of $-b(x)/(-b_1 x)^{2/3a}$ as $x\to\infty$ as a function of a in the "convergent, $\kappa>0$" regime for a number of a values. The curve intersects the abscissa at the value of $a=0.5275$ where $\kappa=0$.

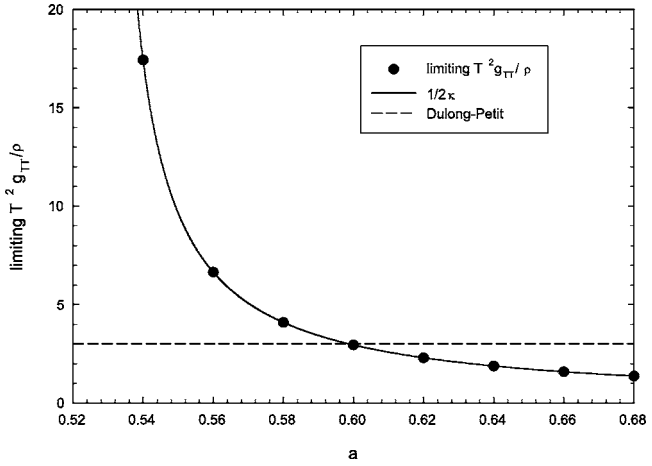

FIG. 10. The limiting $T^2 g_{TT}/\rho$ as a function of a computed numerically from the geometric theory. Values increase as a decreases to 0.5275 where κ goes to zero. Also shown is the function $1/2\kappa$, which appears indistinguishable from the numerical values.

the limiting values are numerically indistinguishable from $1/2\kappa$, and Fig. 10 shows also this function.

I conclude this subsection with the first-order phase transition discussed in Sec. VI. We must first construct fluid and solid curves $(x, b(x))$. The fluid curve is the solution to the geometric equation starting at the origin. The solid curve must be one going to the limit in Theorem 4, including the constant multiplier. There are a number of such curves, and, for simplicity, I pick the analytic curve Eq. (57), which solves the geometric equation exactly for all a. The constant k can be worked out from statistical mechanics using Eq. (48).

With these curves known, the constant pressure relation Eq. (71) yields x_B for any x_A. Figure 11 shows $-b_1 x_B$ as a function of $-b_1 x_A$. Clearly, for $-b_1 x_A < 4.93$ the solid curve has a larger density than the fluid curve, as might be expected physically. Again, the geometric equation does not require a phase transition for this value of a, but it certainly

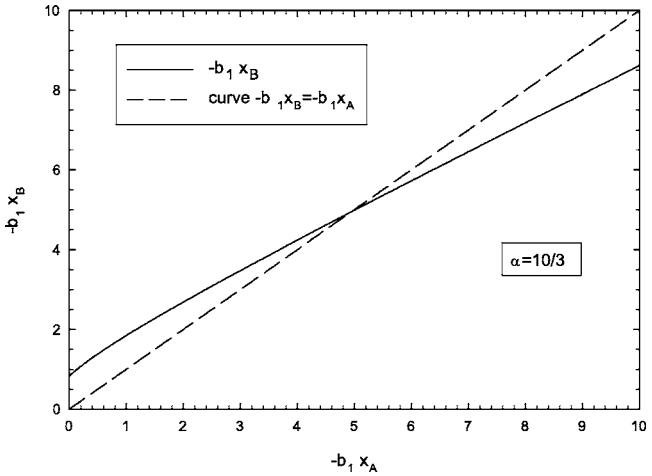

FIG. 11. Corresponding densities x_A and x_B for the fluid and solid curves with $a=3/5$. For $-b_1 x_A < 4.93$, the phase transition corresponds to an increased density.

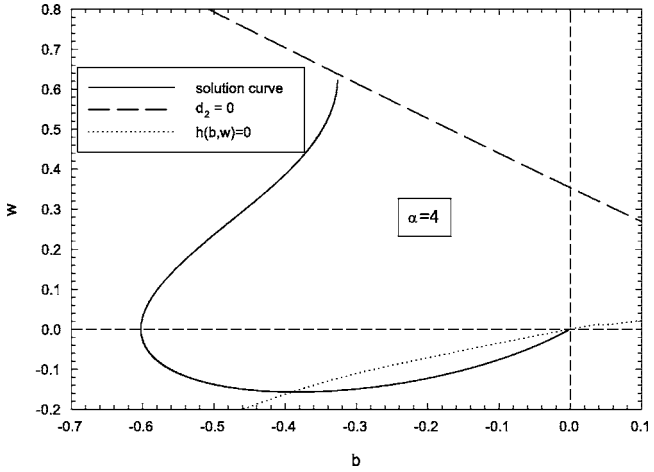

FIG. 12. Solution curve starting at (0, 0) for $a=1/2$. On moving into the third quadrant, it reaches a minimum where it crosses a curve with $h(b,w)=0$. The solution curve then starts back up and eventually encounters a curve of type 1 singularities in the second quadrant where $d_2=0$ in Eq. (43).

allows one. I am not aware of any computer data for this value of a for comparison.

For the solid state curve Eq. (57), $T^2 g_{TT}/\rho$ is everywhere zero; see Sec. IV B. The curve is a straight line in (b,w) space, by Eq. (58). For $a=3/5$, $w=(10/9)b-50/27$. Solution curves starting on the negative w axis at $(0,w)$, with $0>w>-50/27$, go to the solid state limit as $x\to\infty$ with $T^2 g_{TT}/\rho \to 2.9412$, the same as for the fluid curve which starts at (0, 0). Solution curves below the analytic solid state curve have $T^2 g_{TT}/\rho < 0$ and are unphysical.

B. Repulsive potential energy $u(r)=\gamma r^{-4}$

Here, $a=1/2$ and $\kappa=-1/16$ is negative. This a falls into the regime labeled "convergent, $\kappa<0$" in Fig. 4. For $a=1/2$ there are no singularities in the third quadrant or on the negative b axis. Figure 12 shows the solution curve starting at the origin and moving initially into the third quadrant. It reaches a minimum on crossing a curve with $h(b,w)=0$ and moves back up into the second quadrant, where it encounters a curve of type 1 singularities. The metric elements g_{TT} and $g_{\rho\rho}$ are both positive all along this curve, as required by thermodynamic stability.

Obviously, this solution curve cannot go analytically to infinity in the third quadrant in the way expected physically. To make headway, a phase transition is required. Consider solution curves not containing the origin. Figure 13 shows several examples. Solution curves starting close to the origin show the same qualitative behavior as the one in Fig. 12. However, curves starting further away go to infinity in the third quadrant with the same x dependence as in Theorem 4. The straight line solution of Eq. (58) passes through $(0, -8/3)$ and is indicated with an arrow in Fig. 13. It marks the boundary between curves having positive (above) and negative (below) g_{TT}. The solution curves "above" all eventually terminate on the curve of type 1 singular points. The solution curves "below," have negative heat capacity and are hence

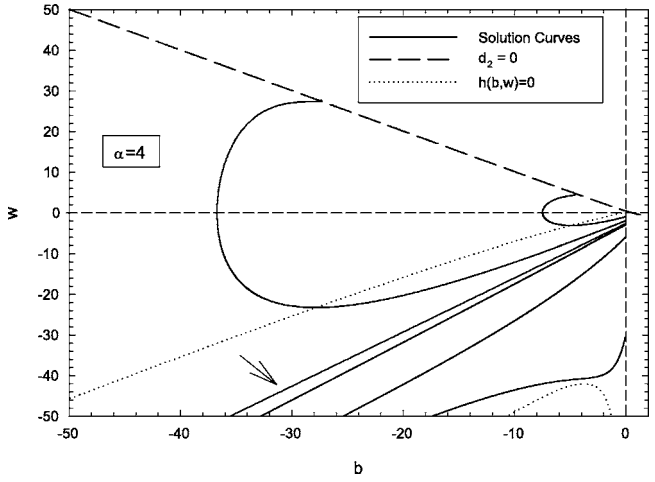

FIG. 13. Solution curves for $a=1/2$ for several cases not containing the origin. The curves are all started on the negative w axis. Those starting at $(b,w)=(0,-1)$ and $(0,-2)$ bottom out, and drift into the second quadrant similar to the curve in Fig. 12. But, the solution curves starting at $(0,-8/3)$, $(0,-3)$, $(0,-6)$, and $(0,-30)$ cross no curve of zeros of $h(b,w)$ and proceed to infinity analytically in the third quadrant in accord with the x dependence in Theorem 4. The arrow points to the straight line solution curve passing through $(0,-8/3)$, which is the boundary between curves of positive (above) and negative (below) g_{TT}.

unphysical. This forces us to make the phase transition by jumping to the straight line solution curve.

Figure 14 shows $-b_1x_B$ as a function of $-b_1x_A$ for the fluid to solid phase transition. For $-b_1x_A<2.55$, the density increases; for larger $-b_1x_A$ it decreases. Remarkably, the point $-b_1x_A=42.8$, where the solution curve terminates on the type 1 singular curve, coincides to within error with the phase transition point from computer simulations with $\alpha=4$ [37]. However, there are other cases where the agreement is not nearly as good, so perhaps this is just a coincidence.

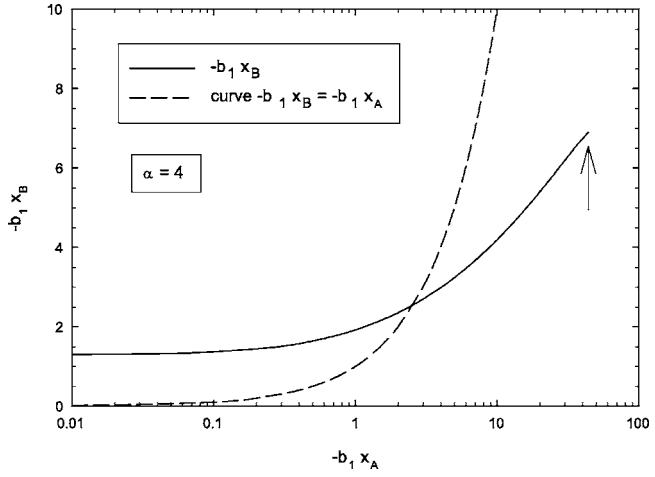

FIG. 14. Corresponding densities x_A and x_B for the fluid and solid curves with $a=1/2$. For $-b_1x_A<2.55$, the phase transition corresponds to an increased density. The arrow marks the point where the solution curve hits the type 1 singularity curve where $d_2=0$ in Eq. (43).

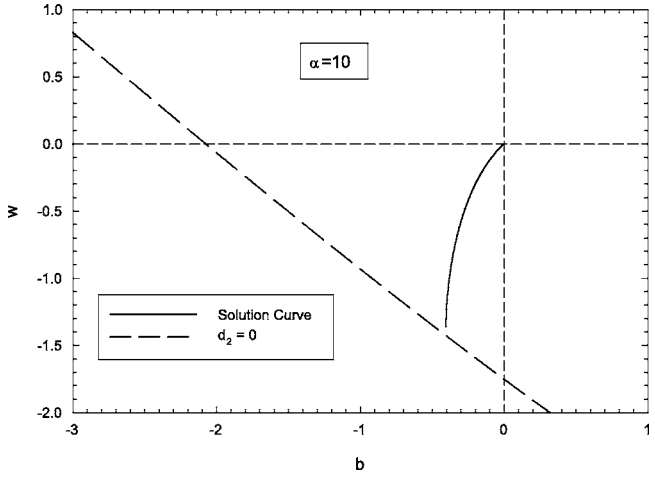

FIG. 15. Solution curve for $a=1/5$ starting at (0,0). It encounters a type 1 singular curve in the third quadrant where $d_2=0$ in Eq. (43). But, there exist solution curves originating on the $-w$ axis and drifting off to infinity in accord with the x dependence in Theorem 4.

The results found in this section are representative of others in the regime $0.3874<a<0.5275$. At $a=0.3874$ the curve of zero denominator of $h(b,w)$ shown in Fig. 12 intersects the origin, which then becomes a type 5 singularity. For smaller values of a, this curve passes through the third quadrant, changing the character of the solution curve. The next subsection looks at such a case.

C. Repulsive potential energy $u(r)=\gamma r^{-10}$

Here, $a=1/5$ and $\kappa=-67/100$. As shown in Fig. 15, the solution curve starting at (0, 0) encounters a type 1 singularity curve in the third quadrant, which is present for all $0<a<0.3874$. Again, one may start curves on the negative w axis which go smoothly to infinity in the third quadrant according to the x dependence in Theorem 4. Such curves included the analytic straight line curve considered above. Thus to construct a solution correct at both low and high densities again involves a phase transition. I tried several values of a in the regime $0<a<0.3874$ and the behavior was qualitatively like that with $a=1/5$.

As $a\to 0$, the type 1 singularity curve goes to negative infinity in the third quadrant. This follows since the intersections of this curve with both the negative b and negative w axes go to minus infinity. The type 1 singularity is thus removed from the third quadrant as $a\to 0$. We look at $a=0$ as a special case in the next subsection.

D. Gas of hard spheres $u(r)=\gamma r^{-\alpha}$, $\alpha\to\infty$

Here, $a=0$ and $\kappa=-1$. The interaction potential energy between a pair of hard spheres, each with radius r_s, is

$$u(r)=\begin{cases}\infty \text{ if } r\leqslant r_s,\\ 0 \text{ if } r>r_s.\end{cases} \tag{74}$$

Write the power-law potential energy Eq. (17) as

$$u(r) = \gamma' \left(\frac{r_s}{r} \right)^{\alpha}, \tag{75}$$

where $\gamma' = \gamma r_s^{-\alpha} > 0$. Clearly, in the limit $\alpha \to \infty$, with γ' held constant, the power-law potential energy acts like the hard sphere potential energy.

For $a=0$, Eqs. (24)–(26) become

$$x = \rho, \tag{76}$$

$$U = \frac{3}{2} N k_B T, \tag{77}$$

and

$$p = \rho k_B T [1 - b(\rho)]. \tag{78}$$

Equation (41) yields

$$h(b,w) = -\left(\frac{2b - 4b^2 + 2b^3 - w - 3bw + 4b^2 w + 2bw^2}{-1 + b} \right). \tag{79}$$

Clearly, there is no type 1 singular curve, other than the irrelevant one $b=1$. This was expected from the previous subsection.

The origin is a type 3 singular point and a series solution for $b(\rho)$ about $\rho=0$ yields

$$p = \rho k_B T \left[1 - (b_1 \rho) + \frac{3}{2}(b_1 \rho)^2 - \frac{13}{5}(b_1 \rho)^3 + \frac{175}{36}(b_1 \rho)^4 + \cdots \right], \tag{80}$$

which, with $b_1 < 0$, shows monotonic growth of $p/\rho k_B T$ with increasing ρ.

As $a \to 0$, the limiting expression in Theorem 2′ has $|b| \to \infty$ and $w/b \to \infty$ for any ρ in the asymptotic regime. This suggests that the solution goes to infinity in the third quadrant, but with w diverging much faster than b. Assuming this, Eq. (79) yields

$$h(b,w) \to -2w^2, \tag{81}$$

and Eqs. (38) and (39) have asymptotic solution

$$b(t) \to k + \frac{1}{2} \ln(t_0 - t), \tag{82}$$

where k and t_0 are constants.

It is evident that $b(t) \to -\infty$ as $t \to t_0$. Correspondingly, by Eqs. (24), (26), and (40), the pressure diverges at a *finite* density:

$$\rho_0 = \frac{1}{|b_1|} \exp(t_0). \tag{83}$$

Contrast this with $a>0$ where the pressure diverges only at infinite density. Pressure divergence at a finite density is physically expected for a gas of hard spheres. It is easy to show from Eq, (82) that the divergence is logarithmic:

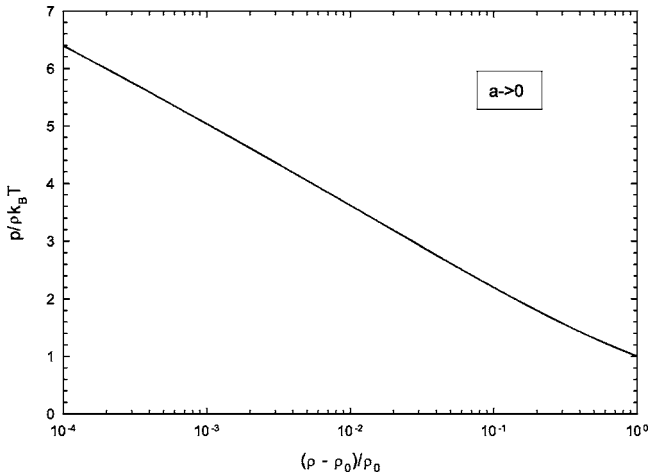

FIG. 16. $p/\rho k_B T$ computed from the geometric equation versus $(\rho_0 - \rho)/\rho_0$. The linearity of the semilogarithmic graph as $\rho \to \rho_0$ demonstrates the logarithmic divergence of $p/\rho k_B T$.

$$\frac{p}{\rho k_B T} \to -\frac{1}{2} \ln\left(\frac{\rho_0 - \rho}{\rho_0} \right). \tag{84}$$

Physically, we expect

$$\rho_0 \sim (2r_s)^{-3}, \tag{85}$$

about the inverse volume of a sphere. For the hard sphere potential energy, Eq. (55) leads to

$$b_1 = -\frac{2\pi}{3} r_s^3, \tag{86}$$

which yields

$$b_1 \rho_0 \sim 0.3. \tag{87}$$

The full numerical solution to the geometric equation starting at the origin results in

$$b_1 \rho_0 = 0.4184, \tag{88}$$

in reasonable agreement with the physical estimate. Figure 16 shows the numerically computed $p/\rho k_B T$ vs. $(\rho_0 - \rho)/\rho_0$. It demonstrates a logarithmic divergence.

VIII. ATTRACTIVE INTERACTIONS

For attractive interactions $\gamma < 0$, statistical mechanics offers no thermodynamic limit. Neither of the integrals Eqs. (20) or (55) converge. But, the geometric theory is not tied to any specific statistical mechanical model and has no integrals obliged to diverge regardless of the thermodynamic state. Assuming that there exists at least one stable state to serve as an initial condition (say, an ideal gas state), we can integrate the geometric equation to find other states. Divergences arise only at singular points or phase transitions.

The case $\gamma < 0$ corresponds to solutions of the geometric equation with $b_1 > 0$. There are two viewpoints to take connecting such solutions to reality. The first is that there is some stable statistical mechanical model yielding the same form of the equations of state Eqs. (25) and (26) as used

here, but with $b(x)$ not connected to microscopic properties by the integral in Eq. (20). It is hard to imagine what form such a statistical mechanics might take since Eq. (20) is reasonably general, but this possibility must at least be considered.

The second viewpoint is that the geometric theory for $b_1>0$ represents quasi-equilibrium states developing far from the eventual collapsed equilibrium reached in a traditional statistical mechanical model. This was the viewpoint taken with the gravity problem considered previously ($\alpha=1$ and $\gamma<0$) [5,42]. There, the constant b_1 was started at 0 (corresponding to a random initial state) and then allowed to increase slowly at constant ρ and T, lowering the free energy as structure forms. This process eventually led to a phase transition, where we would expect the process of structure formation to suffer a "critical slowing down" reflecting the fact that it takes a long time to form structures corresponding to singular thermodynamic functions.

The solution to this gravity problem was applied to galaxy clustering, at a length scale where individual galaxies are point particles interacting with each other via Newtonian gravity. It was demonstrated that the phase transition point corresponds closely to aspects of the observed galaxy distribution [5].

The fact that the geometric theory produces solutions even in cases where statistical mechanics cannot be applied seems to be an advantage. But, I defer further consideration of these interesting problems to future work.

IX. CONCLUSION

In conclusion, I have investigated a class of systems where the Riemannian geometric theory of thermodynamics applies in the form of an ordinary differential equation. This is the first systematic treatment of this theory in interacting systems far from any critical point.

Attention was focused on repulsive power-law systems with exponent $\alpha>3$. A number of points of agreement were found between the geometric theory and statistical mechanics. Not yet entirely satisfactory is the issue of phase transitions from the fluid state to the solid state. Although statistical mechanics offers no definite predictions here, comparison with computer simulations is not convincing. More work is needed.

Despite my attention to cases where a thermodynamic limit exists, and a comparison with statistical mechanics is possible, the geometric theory make predictions also in other cases, including systems with attractive interactions. More work is needed.

ACKNOWLEDGMENTS

I acknowledge Don Colladay, W. G. Hoover, I. Ispolatov, and David Rabson for useful conversations and communications.

[1] H. B. Callen, *Thermodynamics* (Wiley, New York, 1960).
[2] G. Ruppeiner, Phys. Rev. A **20**, 1608 (1979).
[3] G. Ruppeiner, Rev. Mod. Phys. **67**, 605 (1995); **68**, 313(E) (1996).
[4] G. Ruppeiner, Phys. Rev. A **44**, 3583 (1991).
[5] G. Ruppeiner, Astrophys. J. **464**, 547 (1996).
[6] S. Yahikozawa, Phys. Rev. E **69**, 026122 (2004).
[7] J. E. Aman, I. Bengtsson, and N. Pidokrajt, Gen. Relativ. Gravit. **35**, 1733 (2003).
[8] D. C. Brody and A. Ritz, J. Geom. Phys. **47**, 207 (2003).
[9] W. Janke, D. A. Johnston, and R. Kenna, Phys. Rev. E **67**, 046106 (2003).
[10] B. P. Dolan, D. A. Johnson, and R. Kenna, J. Phys. A **35**, 9025 (2002).
[11] R. Balian and P. Valentin, Eur. Phys. J. B **21**, 269 (2001).
[12] H. Oshima, T. Obata, and H. Hara, J. Korean Phys. Soc. **38**, 486 (2001).
[13] K. Kaviani and A. Dalafi-Rezaie, Phys. Rev. E **60**, 3520 (1999).
[14] R. G. Cai and J. H. Cho, Phys. Rev. D **60**, 067502 (1999).
[15] L. Diosi, K. Kulacsy, B. Lukacs, and A. Racz, J. Chem. Phys. **105**, 11220 (1996).
[16] G. Ruppeiner, Phys. Rev. E **57**, 5135 (1998).
[17] L. D. Landau and E. M. Lifshitz, *Statistical Physics* (Pergamon, New York, 1977).
[18] These equations correspond to Eq. (3.38) of Ref. [3].
[19] G. Ruppeiner, Phys. Rev. Lett. **50**, 287 (1983).
[20] G. Ruppeiner, Phys. Rev. A **27**, 1116 (1983).
[21] L. Diosi and B. Lukacs, Phys. Rev. A **31**, 3415 (1985).
[22] L. Tisza and P. M. Quay, Ann. Phys. (N.Y.) **25**, 48 (1963).
[23] S. Amari, *Differential-Geometrical Methods in Statistics*, Lecture Notes in Statistics Vol. 28 (Springer, New York, 1985).
[24] H. Janyszek and R. Mrugala, Phys. Rev. A **39**, 6515 (1989).
[25] D. Laugwitz, *Differential and Riemannian Geometry* (Academic, New York, 1965).
[26] The value of R does, however, depend on which parameter we set aside as the fixed system scale. Here, and in previous works, I have made the natural choice of fixed volume V and fluctuating particle number N. This corresponds to open thermodynamic systems, which are the only ones with no artificial subsystem boundaries to impede the flow of atoms within a system.
[27] B. Widom, Physica (Amsterdam) **73**, 107 (1974).
[28] This equation corresponds to Eq. (6.11) of Ref. [3].
[29] T. Hill, *Statistical Mechanics* (McGraw-Hill, New York, 1956).
[30] The radial distribution function $g(r,T,\rho)$ is denoted by $g(r)$ in Ref. [29] and elsewhere. Here, I explicitly display its dependence on the thermodynamic state.
[31] G. Ruppeiner and J. Chance, J. Chem. Phys. **92**, 3700 (1990).
[32] T. Padmanabhan, Phys. Rep. **188**, 285 (1990).
[33] I. Ispolatov and E. G. D. Cohen, Phys. Rev. Lett. **87**, 210601 (2001); I. Ispolatov and E. G. D. Cohen, Phys. Rev. E **64**, 056103 (2001).
[34] D. Ruelle, *Statistical Mechanics: Rigorous Results* (World Sci-

entific, River Edge, NJ, 1999).
[35] W. C. Saslaw, *Gravitational Physics of Stellar and Galactic Systems* (Cambridge, New York, 1985).
[36] The basic formalism needed to prove this theorem is found at the beginning of Chap. 6 of Ref. [29], in particular Eq. (29.26).
[37] W. G. Hoover, S. G. Gray, and K. W. Johnson, J. Chem. Phys. **55**, 1128 (1971).
[38] C. Kittel, *Introduction to Solid State Physics* (Wiley, New York, 1996).
[39] A. Khurana, Phys. Today **43** (12), 17 (1990).
[40] D. Zwillinger, *Handbook of Differential Equations* (Academic, New York, 1989).
[41] D. A. Young, *Phase Diagrams of the Elements* (Univ. California Press, Berkeley, 1991).
[42] Equation (32) of Ref. [5] contains a typographical error, of no consequence to the rest of the paper. The first term in the first line should have $b \rightarrow -10b$.